Acta Crystallographica Section F
Structural Biology Communications
ISSN 2053-230X

Purification, crystallization and preliminary X-ray crystallographic analysis of human IL-18 and its extracellular complexes

Takeshi Kimura,[a]‡ Naotaka Tsutsumi,[b]‡ Kyohei Arita,[c] Mariko Ariyoshi,[b,d] Hidenori Ohnishi,[a]* Naomi Kondo,[a,e] Masahiro Shirakawa,[b,f] Zenichiro Kato[a,g] and Hidehito Tochio[b]*

[a]Department of Pediatrics, Graduate School of Medicine, Gifu University, Yanagido 1-1, Gifu 501-1194, Japan, [b]Department of Molecular Engineering, Graduate School of Engineering, Kyoto University, Katsura, Nishikyo-ku, Kyoto 615-8510, Japan, [c]Graduate School of Medical Life Science, Yokohama City University, 1-7-29 Suehiro-cho,Tsurumi-ku, Yokohama, Japan, [d]Institute for Integrated Cell-Material Sciences, Kyoto University, Kyoto 606-8501, Japan, [e]Heisei College of Health Sciences, 180 Kurono, Gifu 501-1131, Japan, [f]Core Research of Evolution Science (CREST), Japan Sciences and Technology Agency, Tokyo 102-0076, Japan, and [g]Biomedical Informatics, Medical Information Sciences Division, The United Graduate School of Drug Discovery and Medical Information Sciences, Gifu University, Gifu 501-1194, Japan

‡ Co-first authors.

Correspondence e-mail: ohnishih@gifu-u.ac.jp, tochio@moleng.kyoto-u.ac.jp

Received 10 June 2014
Accepted 22 July 2014

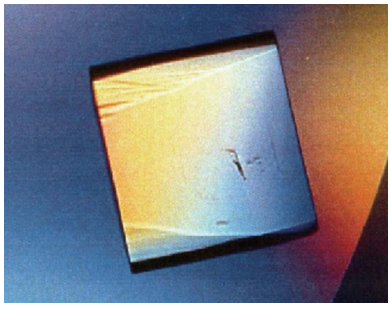

Interleukin-18 (IL-18), a pro-inflammatory cytokine belonging to the interleukin-1 (IL-1) family, is involved in the pathogenesis of autoimmune/autoinflammatory and allergic diseases such as juvenile idiopathic arthritis and bronchial asthma. IL-18 forms a signalling complex with the IL-18 receptor α (IL-18Rα) and β (IL-18Rβ) chains; however, the detailed activation mechanism remains unclear. Here, the IL-18–IL-18Rα binary and IL-18–IL-18Rα–IL-18Rβ ternary complexes were purified and crystallized as well as IL-18 alone. An X-ray diffraction data set for IL-18 was collected to 2.33 Å resolution from a crystal belonging to space group $P2_1$, with unit-cell parameters a = 68.15, b = 79.51, c = 73.46 Å, β = 100.97°. Crystals of both the IL-18 binary and ternary complexes belonging to the orthorhombic space groups $P2_12_12$ and $P2_12_12_1$, respectively, diffracted to 3.10 Å resolution. Unit-cell parameters were determined as a = 135.49, b = 174.81, c = 183.40 Å for the binary complex and a = 72.56, b = 111.56, c = 134.57 Å for the ternary complex.

1. Introduction

IL-18 is a pro-inflammatory cytokine that was first identified as an interferon-γ (IFN-γ)-inducing factor in the sera of endotoxin-injected mice (Okamura *et al.*, 1995). IL-18 not only plays an important role in host defence against microorganisms, but also contributes to the pathogenesis of autoimmune/autoinflammatory and allergic diseases (Nakanishi *et al.*, 2010) such as juvenile idiopathic arthritis (Lotito *et al.*, 2007), familial Mediterranean fever (Simsek *et al.*, 2007), cryopyrin-associated periodic syndrome (Ohnishi *et al.*, 2012), bronchial asthma (Tanaka *et al.*, 2001) and atopic dermatitis (Ohnishi *et al.*, 2003). IL-18 is expressed by various cell types including macrophages, keratinocytes and osteoblasts (Lorey *et al.*, 2004) and belongs to the IL-1 superfamily, sharing structural and functional properties with IL-1β. IL-18 also shares the same signalling cascade with IL-1β. The inflammatory cytokines or stimulants for Toll-like receptors activate intracellular NOD-like receptors such as NLRP3. Activated NLRP3 recruits adaptor protein ASC and caspase-1 precursor (pro-caspase-1); collectively, these proteins form a complex referred to as the inflammasome (Srinivasula *et al.*, 2002). Formation of the inflammasome leads to autocatalytic cleavage of pro-caspase-1, and activated caspase-1 subsequently maturates the IL-18 precursor, which is then secreted outside the cell. To initiate IL-18 intracellular signalling, mature IL-18 is required for the assembly of IL-18Rα and IL-18Rβ. First IL-18 binds to IL-18Rα at the plasma membrane, and then IL-18Rβ binds to the IL-18–IL-18Rα heterodimeric complex (Kato *et al.*, 2003). Assembly of the extracellular region juxtaposes the intracellular Toll-IL-1 receptor (TIR) domains of IL-18Rα and IL-18Rβ, which recruit the adapter molecule MyD88 and sequentially activate IRAKs, TRAF6 and finally NF-κB (O'Neill & Greene, 1998). This signalling cascade then up-regulates the expression of inflammatory cytokines such as IFN-γ. Increased serum levels of IL-18 are frequently correlated with the severity of the autoimmune and autoinflammatory diseases described above. Because of its critical

Table 1
Macromolecule-production information.

Amino acids shown in bold were removed after protease cleavage.

Gene	IL-18	IL-18Rα	IL-18Rβ
Source organism	*Homo sapiens*	*Homo sapiens*	*Homo sapiens*
DNA source	Blood	Blood	Blood
Forward primer	GGATCCATCGAAGGTCGTTACTTTGGCAAGCTTGAATC	GAATTCATGCCCATGTTAAGCGCTATTGTTTTATATGTG-CTTTTGGCGGCGGCGGCGCATTCTGCCTTTGCGGAA-TCTTGTACTTCACGTCCCC	GAATTCATGCCCATGTTAAGCGCTATTGTTTTATATGTG-CTTTTGGCGGCGGCGGCGCATTCTGCCTTTGCGGAG-CGAATTAAAGGATTTAATATTTCAGGTTG
Reverse primer	GAATTCGCTAGTCTTCGTTTTGAACAGTGAAC	GCGGCCGCCTATCTTGTGAAGACGTGGCC	GCGGCCGCTCATCTCTTTTCTTTCAGTTGGACGGAC
Cloning vector	pGEM-T vector	pGEM-T vector	pGEM-T vector
Expression vector	pGEX-4T1	pFastBac1	pFastBac1
Expression host	*E. coli* BL21(DE3)	Sf9 insect cells	Sf9 insect cells
Complete amino-acid sequence of the construct produced	**MSPILGYWKIKGLVQPTRLLLEYLEEKYEEHLYERDEGD-KWRNKKFELGLEFPNLPYYIDGDVKLTQSMAIIRYI-ADKHNMLGGCPKERAEISMLEGAVLDIRYGVSRIAY-SKDFETLKVDFLSKLPEMLKMFEDRLCHKTYLNGDH-VTHPDFMLYDALDVVLYMDPMCLDAFPKLVCFKKRI-EAIPQIDKYLKSSKYIAWPLQGWQATFGGGDHPPKS-DLVPRGSIEGR**YFGKLESKLSVIRNLNDQVLFIDQG-YFGKLESKLSVIRNLNDQVLFIDQGNRPLFEDMTDS-DCRDNAPRTIFIISMYKDSQPRGMAVTISVKCEKIS-TLSCENKIISFKEMNPPDNIKDTKSDIIFFQRSVPG-HDNKMQFESSSYEGYFLACEKERDLFKLILKKEDEL-GDRSIMFTVQNED	**HHHHHHHHLEVLFQ**GPSCTSRPHITVVEGEPFYLKHCSC-GPSCTSRPHITVVEGEPFYLKHCSCSLAHEIETTTK-SWYKSSGSQEHVELNPRSSSRIALHDCVLEFWPVEL-NDTGSYFFQMKNYTQKWKLNVIRRNKHSCFTERQVT-SKIVEVKKFFQITCENSYYQTLVNSTSLYKNCKKLL-LENNKNPTIKKNAEFEDQGYYSCVHFLHHNGKLFNI-TKTFNITIVEDRSNIVPVLLGPKLNHVAVELGKNVR-LNCSALLNEEDVIYWMFGEENGSDPNIHEEKEMRIM-TPEGKWHASKVLRIENIGESNLNVLYNCTVASTGGT-DTKSFILVRKAD	**HHHHHHHHLEVLFQ**GPFNISGCSTKKLLWTYSTRSEEEF-GPFNISGCSTKKLLWTYSTRSEEEFVLFCDLPEPQK-SHFCHRNRLSPKQVPEHLPFMGSNDLSDVQWYQQPS-NGDPLEDIRKSYPHIIQDKCTLHFLTPGVNNSGSYI-CRPKMIKSPYDVACCVKMILEVKPQTNASCEYSASH-KQDLLLGSTGSISCPSLSCQSDAQSPAVTWYKNGKL-LSVERSNRIVVDEVYDYHQGTYVCDYTQSDTVSSWT-VRAVVQVRTIVGDTKLKPDILDPVEDTLEVELGKPL-TISCKARFGFERVFNPVIKWYIKDSDLEWEVSVPEA-KSIKSTLKDEIIERNIILEKVTQRDLRRKFVCFVQN-SIGNTTQSVQLKEKR

role in mediating inflammatory immune responses *in vivo*, IL-18 is normally regulated *via* the naturally occurring IL-18-binding protein (IL-18BP). IL-18BP specifically binds to IL-18 with high affinity, with a dissociation constant of 0.4 n*M*, and prevents IL-18 recognition of IL-18Rα (Dinarello *et al.*, 2013), which is functionally analogous to inhibition of IL-1β signalling by the IL-1β decoy receptor (IL-1RII). Indeed, the potent ability of IL-18 to mediate severe chronic disease has attracted a great deal of interest in the development of new therapeutic reagents that target the IL-18 signalling pathway. However, the structural basis of the IL-18 signalling complex, which can dramatically promote the rational design of IL-18 inhibitory drugs, remains unclear. To this end, we purified and crystallized the IL-18–IL-18Rα binary and IL-18–IL-18Rα–IL-18Rβ ternary complexes as well as the IL-18 monomer; here, we report the preliminary X-ray analysis of each protein.

2. Materials and methods

2.1. Cloning, expression and purification of IL-18, IL-18Rα and IL-18Rβ

IL-18 was overproduced with minor modification of the induction conditions and purified as described previously (Li *et al.*, 2003). Briefly, mature human IL-18 (residues 1–157) fused with a factor Xa recognition site at the N-terminus was cloned into the pGEX 4T-1 vector (GE Healthcare, Little Chalfont, England). IL-18 was expressed as a glutathione *S*-transferase (GST) fusion protein in *Escherichia coli* strain BL21(DE3) with 0.05 m*M* isopropyl β-D-1-thiogalactopyranoside. After GST affinity chromatography and removal of the GST tag by digestion with factor Xa, IL-18 was purified by gel-filtration column chromatography. The extracellular domains of human IL-18Rα (NM_003855, residues 20–329) or IL-18Rβ (NM_003853, residues 15–356) were each cloned separately into the pFastBac1 baculovirus transfer vector (Invitrogen, Carlsbad, California, USA) with an N-terminal signal peptide sequence for Sf9 insect cells, an 8×His tag and a human rhinovirus (HRV) 3C protease cleavage site. Firstly, the coding sequence of each extracellular domain was amplified by PCR with primers containing the signal peptide sequence (Table 1) and then ligated into the pFastBac1 vector between *Eco*RI and *Not*I restriction sites. Secondly, a DNA oligo (48 bp) encoding an 8×His tag and an HRV 3C cleavage site was phosphorylated by T4 kinase (Toyobo, Osaka, Japan) and inserted into the linearized transfer vectors, which were prepared by PCR, using the blunt-end ligation method. Consequently, an 8×His tag cleavable by HRV 3C protease was inserted before the coding sequences. IL-18Rα and IL-18Rβ were expressed using the same protocol. The modified transfer vector was introduced into *E. coli* DH10Bac (Invitrogen) to generate bacmid DNA, which was transfected into Sf9 cells to generate recombinant baculovirus. The baculovirus was then amplified in two cycles. For IL-18 receptor production, Sf9 cell cultures at a density of 2×10^6 cells ml^{-1} were infected with the recombinant baculovirus at a multiplicity of infection (m.o.i.) of 0.1 plaque-forming units (pfu) per cell. Baculovirus-infected Sf9 culture media were harvested after 72 h by centrifugation. The IL-18 receptors were each purified separately using the same chromatographic steps. The receptor secreted from Sf9 cells was collected with ion-exchange columns from the culture media, most impurities were removed using Q Sepharose (GE Healthcare) and the IL-18 receptor in the flowthrough was captured by SP Sepharose (GE Healthcare). After an extensive washing step with 50 m*M* sodium phosphate buffer pH 6.0 containing 50 m*M* sodium chloride, the IL-18 receptor was eluted from an SP Sepharose column with 50 m*M* sodium phosphate buffer pH 6.0 containing 500 m*M* sodium chloride. The pH of the eluate was then adjusted to 7.4 with sodium hydroxide solution and the 8×His-tagged proteins were purified by Ni–NTA agarose (Qiagen, Venlo, Netherlands) chromatography with elution buffer containing an linear gradient of imidazole concentration from 150 to 250 m*M*. After digestion of the N-terminal 8×His tag with HRV 3C protease, the receptor was further purified by size-exclusion chromatography on an Superdex 75 26/60 column (GE Healthcare) with 20 m*M* sodium phosphate buffer pH 7.0 containing 150 m*M* sodium chloride and 0.1 m*M* ethylenediaminetetraacetic acid; the HRV 3C protease was removed in this step.

To obtain the IL-18–IL-18Rα binary and IL-18–IL-18Rα–IL-18Rβ ternary complexes, IL-18, IL-18Rα and IL-18Rβ were mixed in equimolar ratios and purified by gel-filtration chromatography on a Superdex 200 16/60 column with the same buffer as that used in the previous gel-filtration step. Protein elution was monitored at a wavelength of 280 nm. Moreover, we assessed the molecular weights of each protein or protein complex using analytical gel-filtration

Table 2
Crystallization.

Sample	IL-18	IL-18–IL-18Rα	IL-18–IL-18Rα–IL-18Rβ
Method	Vapour diffusion	Vapour diffusion	Vapour diffusion
Plate type	Hanging drop	Hanging drop	Sitting drop
Temperature (K)	277	293	277
Protein concentration (mg ml^{-1})	7	9	10
Buffer composition of protein solution	5 m*M* HEPES–Na pH 7.0, 10 m*M* NaCl	5 m*M* HEPES–Na pH 7.0, 10 m*M* NaCl	5 m*M* HEPES–Na pH 7.0, 10 m*M* NaCl
Composition of reservoir solution	2.5 *M* ammonium sulfate, 100 m*M* bis-tris–HCl pH 7.0	35% PEE 797, 350 m*M* ammonium sulfate, 50 m*M* CAPS pH 9.0 with or without 450 m*M* NDSB-201	18% PEG 4000, 200 m*M* $MgCl_2$, 40 m*M* $[Co(NH_3)_6]Cl_3$, 100 m*M* Tris–HCl pH 7.4
Additive solution	0.25%(*w*/*v*) CHAPS	50 m*M* LysoFos Choline 10 or LysoFos Choline Ether 10	None
Volume ratio of drop† (µl)	0.4:0.4:0.2	With NDSB-201, 1.0:1.0:0; without NDSB-201, 1.0:1.0:0.5	1.0:1.0

† The mixed volume ratio of protein solution:reservoir solution:additive solution.

Table 3
Data collection and processing.

Values in parentheses are for the outer shell.

Molecule	IL-18	IL-18–IL-18Rα	IL-18–IL-18Rα	IL-18–IL-18Rα	IL-18–IL-18Rα–IL-18Rβ
Detergent	CHAPS	NDSB-201	LysoFos Choline Ether 10	LysoFos Choline 10	None
Diffraction source	BL38B1, SPring-8	BL1A, PF	BL5A, PF	BL44XU, SPring-8	BL17A, PF
Wavelength (Å)	1.0000	1.1000	0.9407	0.9000	0.9800
Temperature (K)	100	100	100	100	100
Detector	ADSC Q315	Dectris PILATUS 2M	ADSC Q315	Rayonix MX225HE	ADSC Q270
Crystal-to-detector distance (mm)	300.0	328.7	319.6	300.0	309.6
Software	*XDS*/*SCALA*	*HKL*-2000	*XDS*/*SCALA*	*XDS*/*SCALA*	*HKL*-2000
Space group	$P2_1$	$P6_122$ or $P6_422$	$P2_12_12$	$P2_12_12$	$P2_12_12_1$
a, *b*, *c* (Å)	68.15, 79.51, 73.46	148.05, 148.05, 226.35	136.09, 175.65, 184.57	135.49, 174.81, 183.40	72.56, 111.56, 134.57
α, β, γ (°)	90.00, 100.97, 90.00	90.00, 90.00, 120.00	90.00, 90.00, 90.00	90.00, 90.00, 90.00	90.00, 90.00, 90.00
Theoretical or estimated MW† (kDa)	18.2	70.0	70.0	70.0	119.5
Molecules in asymmetric unit	4	2	6	6	1
V_M (Å^3 Da^{-1})	2.68	2.56	2.63	2.59	2.28
Resolution range (Å)	45.0–2.33 (2.46–2.33)	42.0–3.90 (4.04–3.90)	47.3–3.30 (3.48–3.30)	43.9–3.10 (3.27–3.10)	50.0–3.10 (3.21–3.10)
Total No. of reflections	121376	144429	989916	296079	202352
No. of unique reflections	32990	13981	66776	79180	20587
Completeness (%)	97.8 (97.1)	100 (99.9)	99.4 (99.1)	99.6 (100)	99.9 (99.3)
Multiplicity	3.8 (3.8)	10.3 (10.4)	14.8 (15.3)	3.7 (3.8)	9.8 (9.2)
$\langle I/\sigma(I)\rangle$	20.5 (3.6)	15.2 (2.1)	20.0 (4.5)	14.9 (2.5)	19.8 (2.9)
$R_{r.i.m.}$ (%)	5.7 (46.1)	15.0 (75.6)	14.2 (84.1)	11.7 (67.8)	12.1 (72.3)

† The molecular weights (MW) of the binary and ternary complexes are estimated from the gel-filtration profile because the receptors have heterogeneous N-linked high-mannose glycans. The values are used for calculation of the Matthews coefficient (V_M).

column chromatography. The three proteins were mixed in all possible combinations and each sample was loaded onto a Superdex 200 10/300 GL column (GE Healthcare). Each sample was isocratically eluted at a flow rate of 0.25 ml min^{-1} in 50 m*M* sodium phosphate pH 7.0, 150 m*M* sodium chloride. The molecular masses were estimated using a calibration curve of gel-filtration standards (Bio-Rad, Hercules, California, USA).

2.2. Crystallization

Before crystallization, the protein samples were dialyzed against 5 m*M* HEPES–Na pH 7.0 containing 10 m*M* sodium chloride. Crystallization screening of IL-18 was conducted using the hanging-drop vapour-diffusion method in 24-well plates. Crystals were obtained using an ammonium sulfate-based screening kit (Hampton Research, McLean, Virginia, USA). Subsequently, the crystallization conditions were optimized by adding detergent: 400 nl of 7.0 mg ml^{-1} protein solution was mixed with 400 nl precipitant solution and 200 nl 0.25%(*w*/*v*) CHAPS (Dojindo, Kumamoto, Japan). This mixture was then equilibrated against 500 µl precipitant solution. Crystallization screening of the binary and ternary complexes was carried out using the sitting-drop vapour-diffusion method in 96-well plates, in which 100 nl protein solution was mixed with 100 nl of each precipitant solution. Crystals of the IL-18–IL-18Rα complex were obtained using a pentaerythritol ethoxylate (15/4 EO/OH, PEE 797)-based screening kit (Jena Bioscience, Jena, Germany), while the IL-18–IL-18Rα–IL-18Rβ ternary complex was crystallized using a polyethylene glycol (PEG) 4000-based screening kit (Jena Bioscience). The crystallization conditions for both complexes were optimized by screening various detergents and additives. Crystallizations with optimized conditions were scaled up using the hanging-drop or sitting-drop vapour-diffusion method with 24-well plates in which 1 µl protein solution and 1 µl precipitant solution were typically mixed with or without 0.5 µl detergent. Crystallization drops of the IL-18–IL-18Rα complex were immediately equilibrated with 500 µl precipitant solution. Crystallization of the IL-18–IL-18Rα–IL-18Rβ complex required a dehydration step prior to vapour diffusion, in which the crystallization drops were air-dried for 6 h at 293 K and subsequently placed over reservoir chambers filled with 200 µl of each precipitant solution. Crystallization plates were incubated under protection from light at 277 K for IL-18 and IL-18–IL-18Rα–IL-18Rβ or 293 K for IL-18–IL-18Rα. The final conditions are summarized in Table 2.

2.3. X-ray diffraction data collection and processing

The crystals from each precipitant solution (including detergents) were flash-cooled in liquid nitrogen with cryoprotectant solutions containing 20%(*w*/*v*) glycerol (IL-18 and IL-18–IL-18Rα–IL-18Rβ)

or 20%(*w*/*v*) glucose (IL-18–IL-18Rα). X-ray diffraction data sets were collected at 100 K using the synchrotron beamlines at SPring-8, Harima, Japan or Photon Factory (PF), Tsukuba, Japan. The intensity data were processed using *XDS* (Kabsch, 2010) and *SCALA* (Evans, 2006) or *HKL*-2000 software (Otwinowski & Minor, 1997). When the *XDS* and *SCALA* software were used, the space group was determined using *POINTLESS* (Evans, 2006). The crystallographic data-collection statistics for IL-18, IL-18–IL-18Rα and IL-18–IL-18Rα–IL-18Rβ are summarized in Table 3. For the IL-18–IL-18Rα crystals, the statistics with three detergents NDSB-201 (Merck, Whitehouse Station, New Jersey, USA), LysoFos Choline Ether 10 (Affymetrix, Santa Clara, California, USA) and LysoFos Choline 10 (Affymetrix) are shown to indicate the improvement in the data quality.

3. Results and discussion

3.1. Reconstitution of the extracellular IL-18 signalling complex

We previously established a bacterial overexpression and purification system for IL-18 (Li *et al.*, 2003). For structural analysis of the IL-18-mediated signalling complexes, we used a baculovirus expression system to obtain sufficient amounts of the IL-18Rα and IL-18Rβ receptors for crystallization experiments. Each receptor expressed from Sf9 cells was purified by three chromatographic steps: ion-exchange, metal-affinity and gel-filtration chromatography using Q and SP Sepharose, Ni–NTA agarose (Figs. 1*a* and 1*b*) and Superdex 75 26/60 (Figs. 1*c* and 1*d*). Finally, ∼4 mg IL-18Rα and ∼1 mg IL-18Rβ protein with a purity greater than 90% were obtained from 1 l

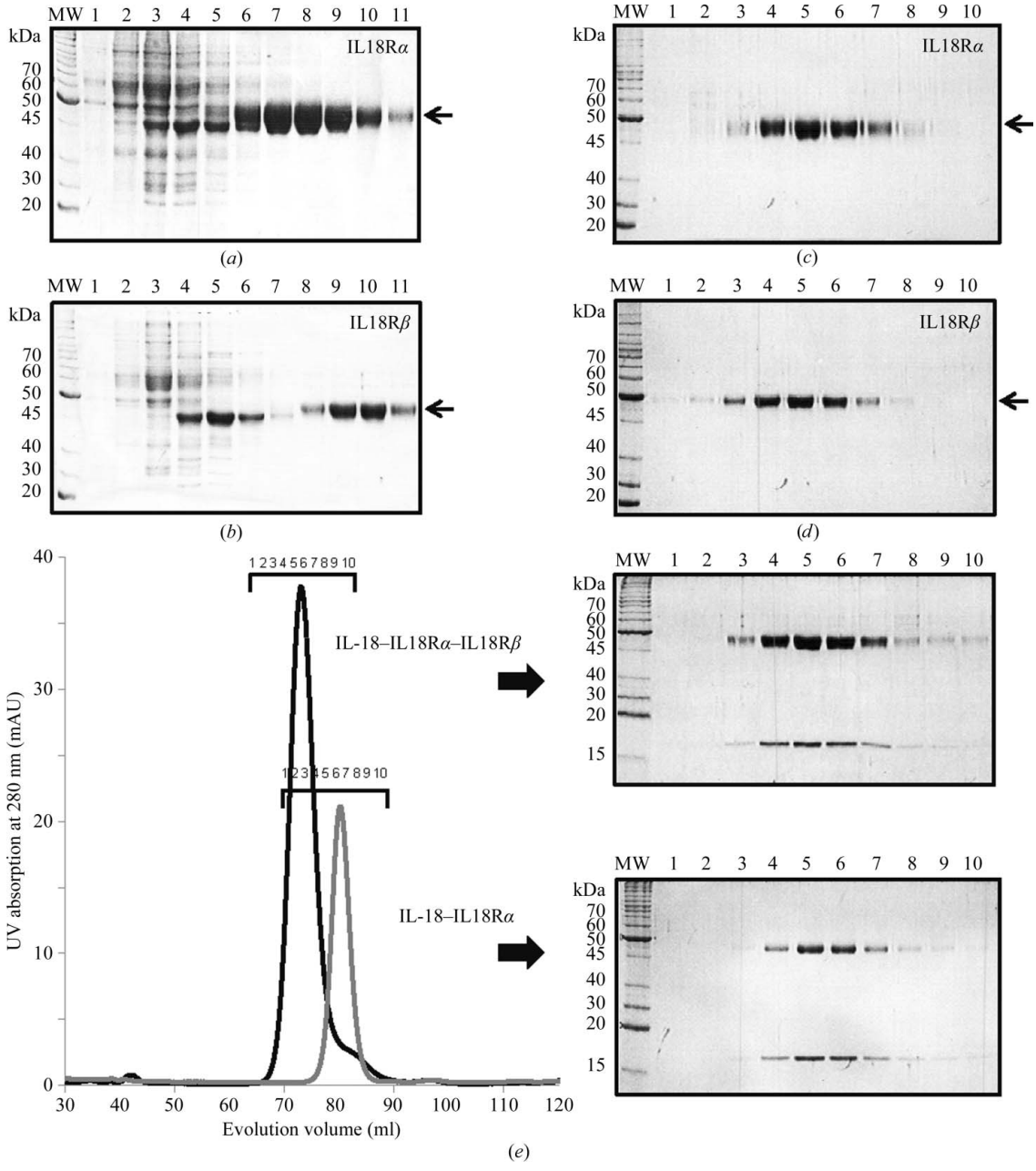

Figure 1
SDS–PAGE analysis of each purification stage. Elution fractions of (*a*) IL-18Rα and (*b*) IL-18Rβ from an Ni–NTA agarose column with an imidazole linear gradient. Peak fractions of (*c*) IL-18Rα and (*d*) IL-18Rβ on size-exclusion chromatography. (*e*) Elution profiles of the IL-18 binary (gray) and IL-18 ternary (black) complexes on size-exclusion chromatography; the peak fractions were analyzed by SDS–PAGE.

Sf9 cell culture (Figs. 1*c* and 1*d*), while ∼5 mg of IL-18 was obtained from 1 l *E. coli* culture. To form the binary and ternary complexes, purified IL-18, IL-18Rα and IL-18Rβ were mixed and loaded onto a Superdex 200 16/60 column and each complex was isocratically eluted as a single peak (Fig. 1*e*).

The IL-18 ternary complex was previously reported to assemble in a hierarchical order (Kato *et al.*, 2003). We confirmed this finding and its stoichiometry using analytical gel-filtration column chromatography with purified recombinant proteins. Formation of a ternary complex (MW 119.5 kDa) with 1:1:1 stoichiometry was clearly observed (Fig. 2*a*). In the absence of IL-18Rβ (MW 51.5 kDa), IL-18Rα (MW 61.4 kDa) and IL-18 (MW 18.6 kDa) co-eluted as a complex with an estimated molecular mass of 70.0 kDa, suggesting stable 1:1 complex formation (Fig. 2*a*). In contrast, the IL-18Rβ receptor did not show complex formation with IL-18Rα or IL-18 alone (Figs. 2*b* and 2*c*). Thus, our data clearly demonstrate that the IL-18–IL-18Rα binary complex is required for the binding of IL-18Rβ. Both the IL-18–IL-18Rα and IL-18–IL-18Rα–IL-18Rβ complexes were subjected to crystallization screening.

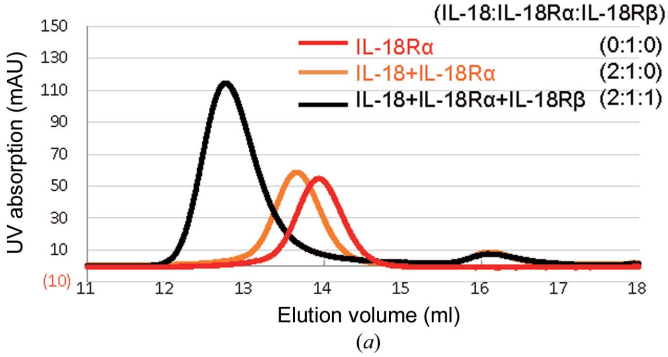

(*a*)

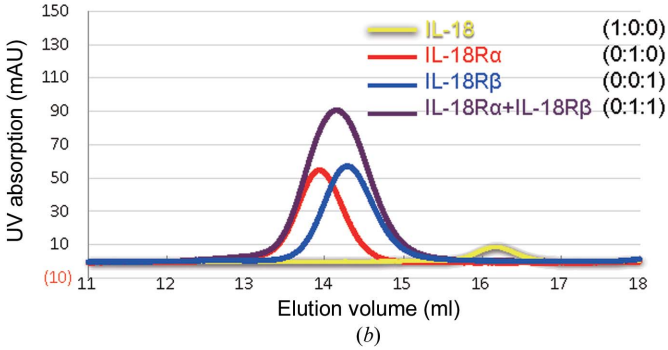

(*b*)

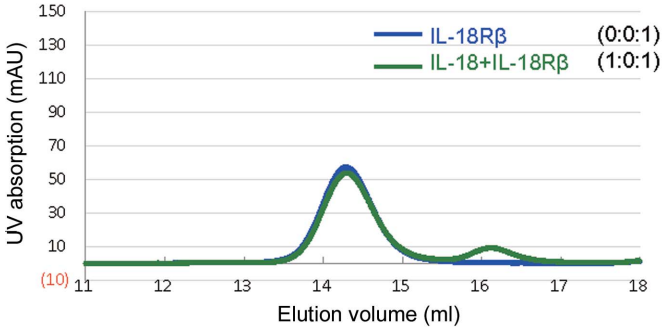

(*c*)

3.2. Crystallization and preliminary crystallographic analysis

Optimized crystallization conditions are summarized in Table 2. Single crystals of IL-18 with typical dimensions of 200 × 200 × 200 µm (maximum dimensions 300 × 300 × 300 µm) appeared within one week at 277 K (Fig. 3*a*). Crystals of IL-18–IL-18Rα were obtained with various detergents as indicated in Table 2. Spherical moss-like crystals were initially obtained, but three single-crystal forms appeared in the presence of different detergents within a few days at 293 K; these detergents were NDSB-201 (Fig. 3*b*), LysoFos Choline Ether 10 (Fig. 3*c*) and LysoFos Choline 10 (Fig. 3*d*). A single crystal of IL-18–IL-18Rα–IL-18Rβ with dimensions of 50 × 50 × 300 µm appeared within a few weeks at 277 K (Fig. 3*e*).

Crystals of IL-18 diffracted to 2.33 Å resolution and belonged to space group $P2_1$, with unit-cell parameters a = 68.15, b = 79.51, c = 73.46 Å, β = 100.97°. The IL-18–IL-18Rα complex crystals obtained with NDSB-201 or LysoFos Choline Ether 10 diffracted to 3.90 and 3.30 Å resolution, respectively, and a complete data set was collected for each. Of the three crystal forms, the crystal obtained with LysoFos Choline 10 yielded a complete data set at the highest resolution, 3.10 Å, and belonged to space group $P2_12_12$, with unit-cell parameters a = 135.49, b = 174.81, c = 183.40 Å. The crystal of the IL-18–IL-18Rα–IL-18Rβ complex diffracted to 3.10 Å resolution and belonged to space group $P2_12_12_1$, with unit-cell parameters a = 72.56, b = 111.56, c = 134.57 Å. Crystallographic data and X-ray data-collection statistics are summarized in Table 3. Further structural determination is in progress.

X-ray data collection was supported by SPring-8 (Harima, Japan), the Photon Factory (Tsukuba, Japan) and the Platform for Drug Discovery, Informatics and Structural Life Science (Japan). We thank T. Tsunaka (Kyoto University) for his support in the use of beamline

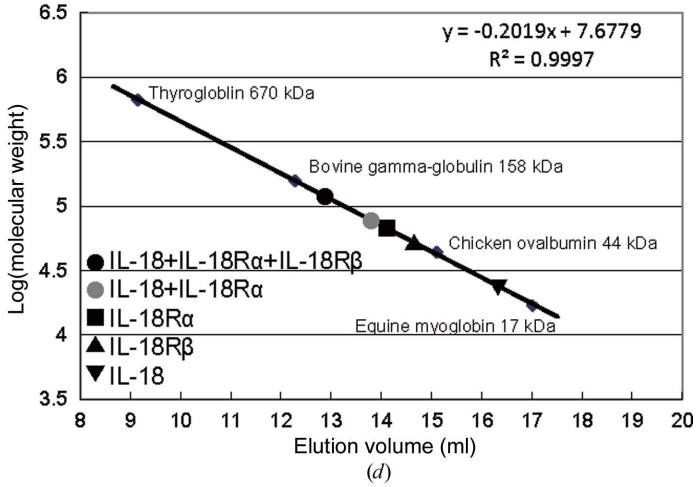

(*d*)

	kDa
IL-18	18.6
IL-18Rα	61.4
IL-18Rβ	51.5
IL-18+IL-18Rα	70.0
IL-18+IL-18Rα+IL-18Rβ	119.5

(*e*)

Figure 2
Gel-filtration profiles for recombinant IL-18, IL-18Rα and IL-18Rβ and their mixtures in all possible combinations. IL-18 and its receptors were mixed at the ratios indicated. (*a*) The typical trace for the binary IL-18–IL-18Rα complex (orange) and ternary IL-18–IL-18Rα–IL-18Rβ complex (black). (*b*) The elution profile for a 1:1 mixture of IL-18Rα and IL-18Rβ (purple) overlaid with that for each receptor alone (red or blue). (*c*) The IL-18 and IL-18Rβ mixture (green) eluted in two separated peaks. (*d*) The elution volumes for IL-18, IL-18Rα, IL-18Rβ and its complexes were plotted against the calibration line. (*e*) A summary of the deduced molecular weights.

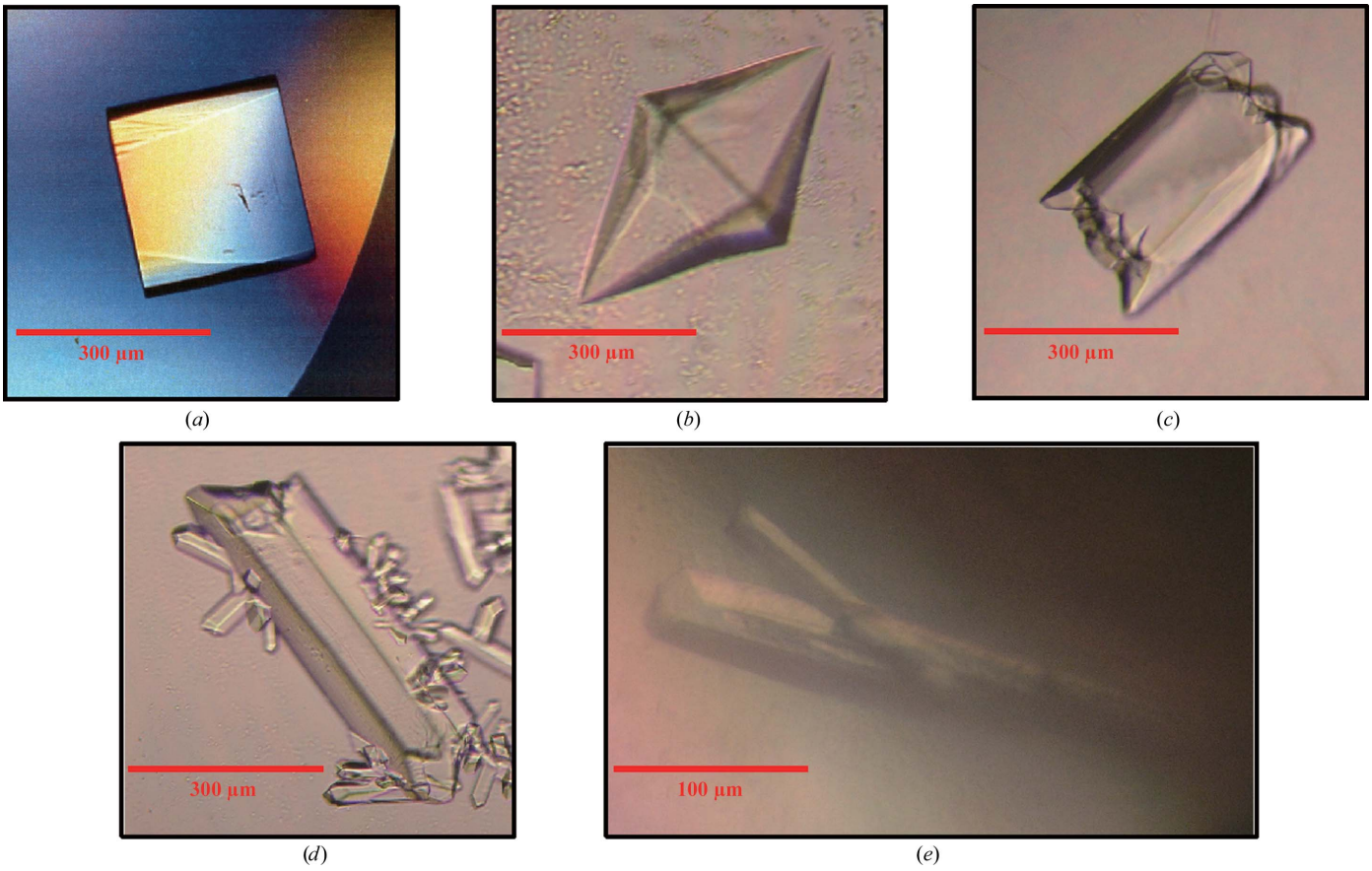

Figure 3
Crystals of IL-18 alone and its extracellular complexes. (*a*) A crystal of IL-18. (*b*) A hexagonal crystal of IL-18–IL-18Rα obtained with NDSB-201. (*c*, *d*) Orthogonal crystals of IL-18–IL-18Rα obtained with (*c*) LysoFos Choline Ether 10 and (*d*) LysoFos Choline 10. (*e*) Crystals of IL-18–IL-18Rα–IL-18Rβ.

BL44XU at SPring-8. We also thank N. Kawamoto, K. Tsuji, M. Yamamoto and K. Kasahara (Gifu University) for their technical assistance. Affymetrix Inc. provided us with discontinued detergents. This work was supported by JSPS KAKENHI Grant Number 22370038 to HT, Grant-in-Aid for JSPS Fellows to NT, and Health and Labour Science Research Grants for Research on Intractable Diseases from the Ministry of Health, Labour and Welfare to HO.

References

Dinarello, C. A., Novick, D., Kim, S. & Kaplanski, G. (2013). *Frontiers Immunol.* **4**, 289.
Evans, P. (2006). *Acta Cryst.* D**62**, 72–82.
Kabsch, W. (2010). *Acta Cryst.* D**66**, 125–132.
Kato, Z., Jee, J., Shikano, H., Mishima, M., Ohki, I., Ohnishi, H., Li, A., Hashimoto, K., Matsukuma, E., Omoya, K., Yamamoto, Y., Yoneda, T., Hara, T., Kondo, N. & Shirakawa, M. (2003). *Nature Struct. Biol.* **10**, 966–971.
Li, A., Kato, Z., Ohnishi, H., Hashimoto, K., Matsukuma, E., Omoya, K., Yamamoto, Y. & Kondo, N. (2003). *Protein Expr. Purif.* **32**, 110–118.
Lorey, S. L., Huang, Y. C. & Sharma, V. (2004). *Clin. Exp. Immunol.* **136**, 456–462.
Lotito, A. P. N., Campa, A., Silva, C. A. A., Kiss, M. H. B. & Mello, S. B. V. (2007). *J. Rheumatol.* **34**, 823–830.
Nakanishi, K., Tsutsui, H. & Yoshimoto, T. (2010). *Allergol. Int.* **59**, 137–141.
Ohnishi, H., Kato, Z., Watanabe, M., Fukutomi, O., Inoue, R., Teramoto, T. & Kondo, N. (2003). *Allergol. Int.* **52**, 123–130.
Ohnishi, H., Teramoto, T., Iwata, H., Kato, Z., Kimura, T., Kubota, K., Nishikomori, R., Kaneko, H., Seishima, M. & Kondo, N. (2012). *J. Clin. Immunol.* **32**, 221–229.
Okamura, H. *et al.* (1995). *Nature (London)*, **378**, 88–91.
O'Neill, L. A. & Greene, C. (1998). *J. Leukoc. Biol.* **63**, 650–657.
Otwinowski, Z. & Minor, W. (1997). *Methods Enzymol.* **276**, 307–326.
Simsek, I., Pay, S., Pekel, A., Dinc, A., Musabak, U., Erdem, H. & Sengul, A. (2007). *Rheumatol. Int.* **27**, 807–811.
Srinivasula, S. M., Poyet, J.-L., Razmara, M., Datta, P., Zhang, Z. & Alnemri, E. S. (2002). *J. Biol. Chem.* **277**, 21119–21122.
Tanaka, H., Miyazaki, N., Oashi, K., Teramoto, S., Shiratori, M., Hashimoto, M., Ohmichi, M. & Abe, S. (2001). *J. Allergy Clin. Immunol.* **107**, 331–336.